Second order closure for stratified convection: bulk region and overshooting

2011 J. Phys.: Conf. Ser. 318 042018

(http://iopscience.iop.org/1742-6596/318/4/042018)

Second order closure for stratified convection: bulk region and overshooting

L. Biferale[1,2], F Mantovani[3], M. Pivanti[4], F. Pozzati[5], M Sbragaglia[1], A. Scagliarini[6], S.F. Schifano[4], F. Toschi[2,7,8], R. Tripiccione[4]

[1] Dept. Physics and INFN University of Rome, Tor Vergata, Italy
[2] Department of Applied Physic Eindhoven University of Technology, The Netherlands
[3] Deutsches Elektronen Synchrotron (DESY), Zeuthen, Germany
[4] University of Ferrara and INFN, Ferrara, Italy
[5] Fondazione Bruno Kessler Trento, Trento, Italy
[6] Department of Fundamental Physics, University of Barcelona, Barcelona, Spain
[7] Department of Mathematics and Computer Science and J.M. Burgers Centre for Fluid Dynamics, Eindhoven University of Technology, The Netherlands
[8] CNR, Istituto per le Applicazioni del Calcolo,Rome, Italy

E-mail: biferale@roma2.infn.it

Abstract. The parameterization of small-scale turbulent fluctuations in convective systems and in the presence of strong stratification is important for many applied problems in oceanography, atmospheric science and planetology. In the presence of stratification, both bulk turbulent fluctuations and inversion regions, where temperature, density –or both– develop highly nonlinear mean profiles, are crucial. We present a second order closure able to reproduce *simultaneously* both bulk and boundary layer regions. We test it using high-resolution state-of-the-art 2D numerical simulations in a Rayleigh-Taylor convective and stratified belt for values of the Rayleigh number, up to $Ra \sim 10^9$. The system is confined by the existence of an adiabatic gradient. Our numerical simulations are performed using a thermal Lattice Boltzmann Method (Sbragaglia et al, 2009) able to reproduce the Navier-Stokes equations for momentum, density and internal energy (see also (Biferale et al, 2011b) for an extension to a case with forcing on internal energy). Validation of the method can be found in (Biferale et al, 2010; Scagliarini et al, 2010). Here we present numerical simulations up to 4096×10000 grid points obtained on the QPACE supercomputer (Goldrian et al, 2008).

1. Introduction

Parameterization of convective regions in presence of strong stratification is interesting for the evolution of the convective boundary layer in different applied and fundamental fields as atmospheric science (Siebesma et al, 2007), stellar convection (Canuto & Christensen-Dalsgaard, 1998; Ludwig et al, 2006; Trampedach, 2010) and oceanography (Large et al, 1994; Burchard & Bolding, 2001; Canuto et al, 2002; Wirth & Barnier, 2008). The problem is also theoretically important because of the interplay between buoyancy and turbulence at the edge between a convective region and a stable stratified volume above/below it. Due to turbulent activity, temperature blobs tend to enter the stratified region, producing an inversion in the energy balance: kinetic energy is indeed lost, potential energy is increased (see Fig. 1). Recent studies have shown that, in the absence of strong stratification, mixing length theory based on Prandtl

or Spiegel closure works very well in situations as different as for the case of Rayleigh-Taylor systems (Boffetta et al, 2010) or in fluid mixing by gravity currents (Odier et al, 2009).

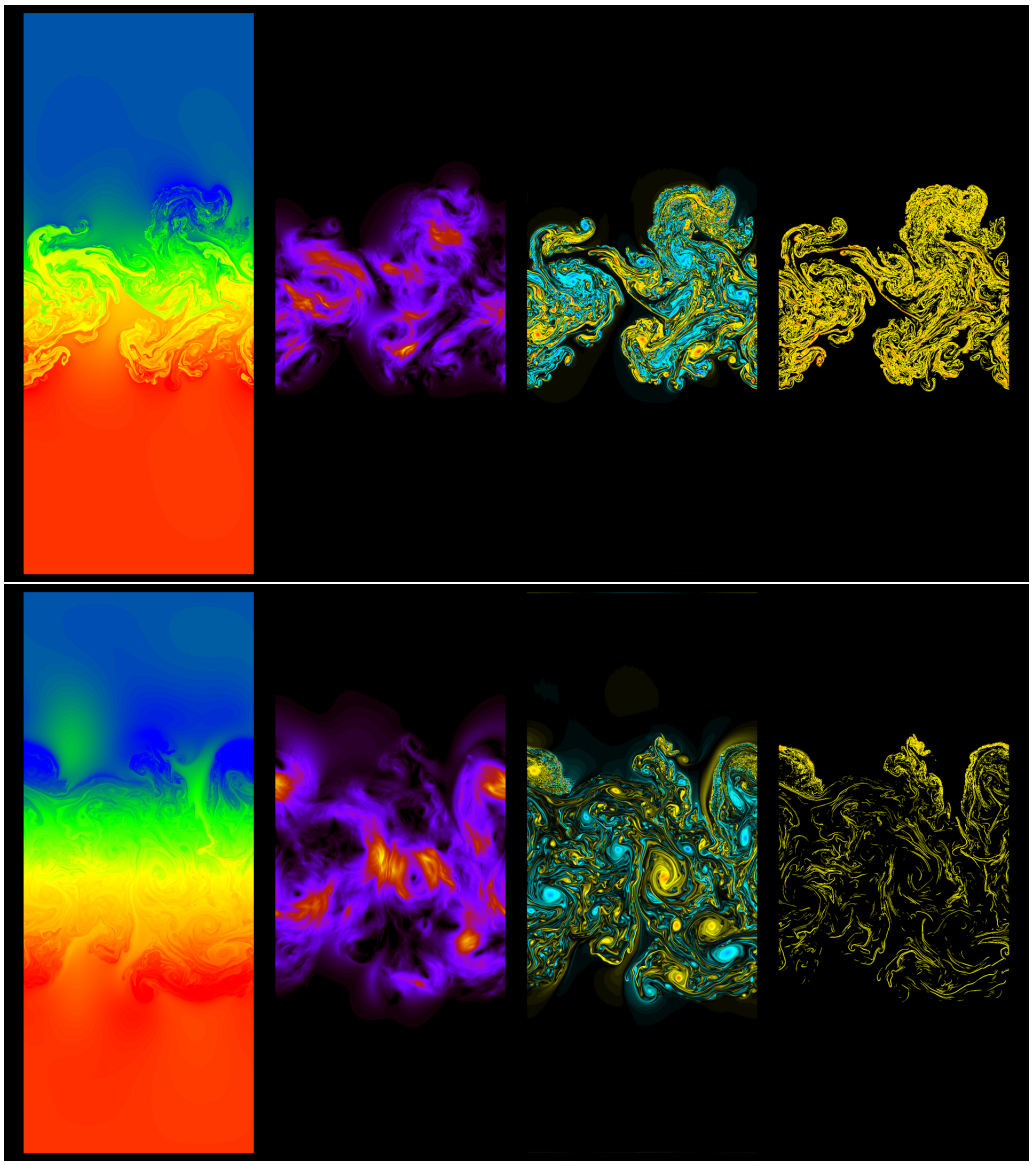

Figure 1. 4 snapshots of the RT evolution at two different times (RUN B with strong stratification). From left to righ: temperature; total kinetic energy; vorticity; amplitude of temperature gradients. Top four snapshot are taken at $t = 5t_{RT}$ bottom four snapshots at $t = 10t_{RT}$, i.e. at the moment of the arrest and after it, respectively. Notice how mixing layer does not evolve anymore. After the evolution halted, only temperature gradients show a clear depletion (fourth column). See also figure 4 for the global evolution of the mixing layer.

When strong stratification stops the evolution of the mixing profile, an overshooting region with temperature inversion develops and local closures fail. The situation can be visualized in the 4 panels of Fig. 1 where we plot temperature, kinetic energy, vorticity and temperature gradients of a Rayleigh-Taylor system whose evolution has been stopped by stratification (Biferale et al, 2011a; Lawrie & Dalziel, 2011). Here, the mean temperature profile is linear in the bulk and

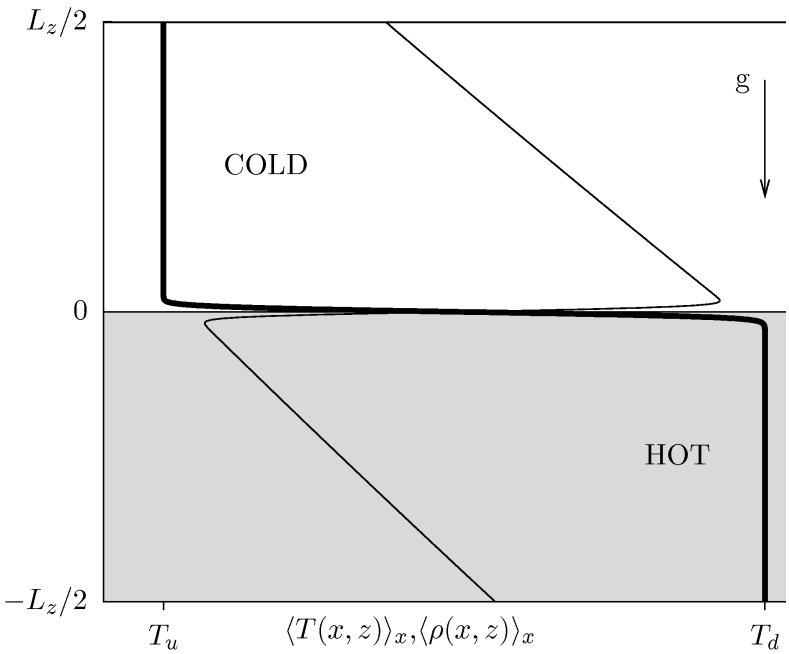

Figure 2. Initial vertical density and temperature configuration for the RT experiment.

it develops two –symmetric– overshooting regions at the edge between the turbulent boundary layer and the fluid at rest with the heat flux inverting sign (Biferale et al, 2011a).

In this proceedings we first briefly review a closure for the evolution of the mixing layer, able to capture both the initial transient (free of any stratification effect) and the late slowing down and stopping due to stratification effects. Then, we present new data showing that our is also able to reproduce the late decay state, many characteristic times after the evolution stopped, where we observe a slow kinetic energy decay (typical of 2D systems where bulk kinetic energy is slowly dissipated).

The main idea of the closure developed in (Biferale et al, 2011a) is to go beyond single point closure for the mean temperature evolution, and closing only for second order quantities: the Reynolds stresses, the heat flux and temperature fluctuations, see e.g. (Burchard & Bolding, 2001). In (Biferale et al, 2011a) we tested the closure against state-of-the-art numerical simulations at high resolution. We choose to work in a 2D geometry to maximize the capability to get quantitative measurements at high Reynolds and Rayleigh numbers. Our numerical simulations are performed using a thermal Lattice Boltzmann Method (Sbragaglia et al, 2009) able to reproduce the Navier-Stokes equations for momentum, density and internal energy. Validation of the method can be found in (Biferale et al, 2010; Scagliarini et al, 2010). We investigate two different set-up, one with weak stratification, i.e. the usual RT evolution (RUN A) and a second one with strong stratification (RUN B). Table I provides details of numerics obtained running on the QPACE supercomputer (Goldrian et al, 2008; Belletti et al, 2008). We discuss the case of an ideal gas and at small Mach number, with the equation of state $P = \rho T$. In this case, the main effect of stratification is limited to the presence of an adiabatic gradient affecting the evolution of temperature (Spiegel, 1965). The equations are the following: (double indexes are summed):

$$\begin{cases} \partial_t u_i + u_j \partial_j u_i = -\frac{\partial_i p}{\rho_m} - \delta_{i,z} g \frac{\theta}{T_m} + \nu \partial_{jj} u_i; & i = x, z \\ \partial_t T + u_j \partial_j T - u_z \gamma = \kappa \partial_{jj} T; \end{cases} \tag{1}$$

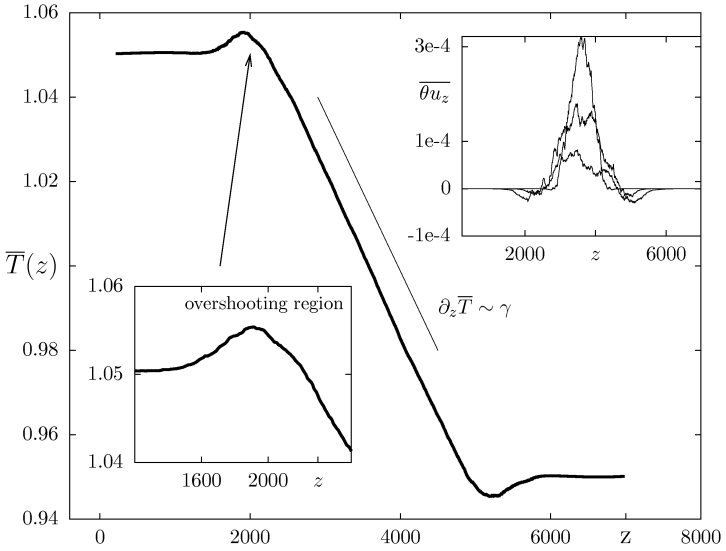

Figure 3. Strong stratification, RUN (B). Mean temperature profile $\overline{T}(z)$ after the RT evolution has stopped at the adiabatic slope (solid line). Bottom left panel: zoom of the overshooting region, with temperature inversion. Top right inset: heat flux profile $\overline{u_z\theta}(z)$ at three times before, during and after stopping: two regions develop with negative heat flux in correspondence of the temperature overshooting.

	L_x	L_z	γ	Ra_{max}	N_{conf}	L_γ	t_{RT}
RUN (A)	4096	10000	$-1 \cdot 10^{-5}$	$8 \cdot 10^9$	18	10000	$6.4 \cdot 10^4$
RUN (B)	3072	7200	$-4.2 \cdot 10^{-5}$	$3 \cdot 10^9$	11	2408	$2.7 \cdot 10^4$

Table 1. Run (A): weak stratification. Run (B) strong stratification. Adiabatic gradient: $\gamma = -g/c_p$; $c_p = 2$. Adiabatic length in grid units: $L_\gamma = \Delta T/|\gamma|$, $\Delta T = T_{down} - T_{up}$, $T_m = (T_{down} + T_{up})/2$ and $T_{up} = 0.95$, $T_{down} = 1.05$. Rayleigh number in presence of stratification is defined as (Spiegel, 1965): $Ra(t) = gL(t)^4(\Delta T/L(t) + \gamma)/(\nu\,\kappa)$). Maximal value is obtained when $L(t) = 3/4L_\gamma$. Number of independent runs with random initial perturbation: N_{conf}. Atwood number $= At = \Delta T/(2\,T_m) = 0.05$. Characteristic time scale, $t_{RT} = \sqrt{L_x/(gAt)}$.

where p is the deviation of pressure from the hydrostatic profile, $p = P - P_H$ and $\partial_z P_H = -g\rho_H$, T_m and ρ_m are the mean temperature and density in the system, g is gravity and the adiabatic gradient is given by its ideal gas expression $\gamma = -g/c_p$ with c_p the specific heat. In this *Boussinesq* approximation (Spiegel, 1965) for stratified flows, momentum is forced only by temperature fluctuations $\theta = T - \bar{T}$ where we use the symbol $\overline{(\cdot)}$ to indicate an average over the horizontal statistically-homogeneous direction. The initial configuration is given by two regions of cold (top) and hot (bottom) fluids prepared in the two half volumes of our cell (see Fig.2); turbulence is triggered by a small perturbation of the interface between them (Sharp, 1984).
From (1), one easily derives the equations for the mean temperature profile, total kinetic energy,

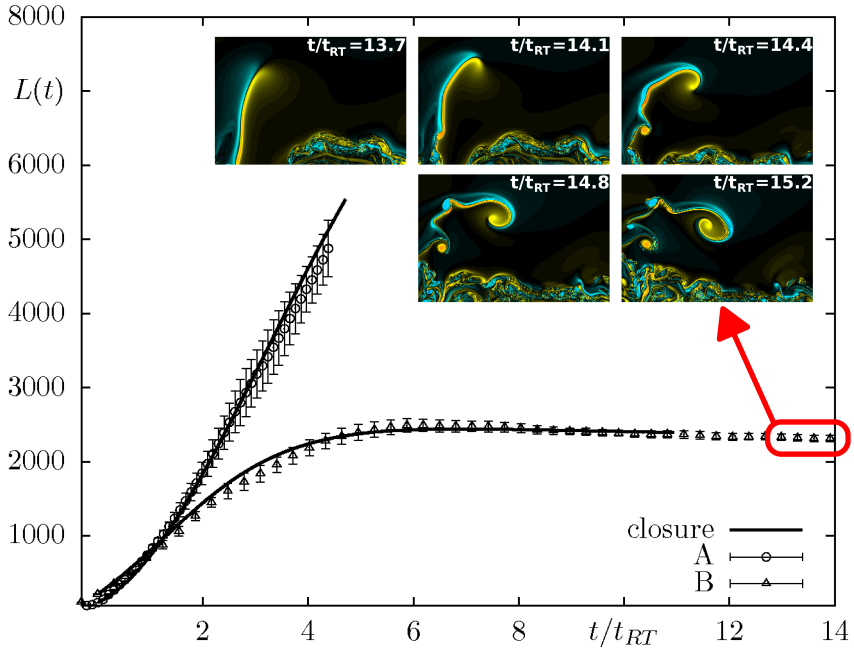

Figure 4. Evolution of the mixing layer extension $L(t)$ for both run (A) and (B). Notice the stop by stratification effects for the latter. Solid lines correspond to the second closure prediction for the mixing length evolution obtained with the choice $[1.45, 4.5]$ (run A) and $[0.3, 6.5]$ (run B) for the parameters $[b_\theta, b_{\theta u_z}]$ (see text). We also show 5 consecutive snapshots of the overshooting region highlighting the formation of a turbulent plume trying to enter the stable region and rejected back by gravitational forces.

heat flux and temperature fluctuations:

$$\begin{cases} \partial_t \overline{T} + \partial_z \overline{u_z \theta} = \kappa \partial_{zz} \overline{T} \\ \frac{1}{2}\partial_t \overline{\theta^2} + \frac{1}{2}\partial_z \overline{\theta^2 u_z} + \overline{u_z \theta}(\partial_z \overline{T} - \gamma) = \kappa \overline{\theta \partial_{jj} \theta} \\ \frac{1}{2}\partial_t \overline{u^2} + \partial_z [\overline{u^2 u_z} + \overline{u_z p}] = -g\overline{\theta u_z} - \epsilon_\nu \\ \partial_t \overline{\theta u_z} + \partial_z [\overline{\theta u_z^2} + \overline{\theta p}] = -g\overline{\theta^2} + \beta(z)\overline{u_z^2} - \epsilon_{\theta,u_z} \end{cases} \tag{2}$$

where $u^2 = u_x^2 + u_z^2$, $\beta(z) = (\partial_z \overline{T} - \gamma)$, and the dissipative terms are: $\epsilon_{\theta,u_z} = (\nu + \kappa)\overline{\partial_i \theta \partial_i u_z}$, $\epsilon_\theta = \kappa \overline{\partial_i \theta \partial_i \theta}$, $\epsilon_\nu = \nu \overline{\partial_i u_j \partial_i u_j}$. These equations are exact, except for boundary dissipative contributions as for example, $\kappa \partial_z \overline{\theta \partial_z \theta}$ which are irrelevant when $\kappa, \nu \to 0$ in absence of walls. From the second of (2) it is evident that temperature fluctuations are not forced anymore as soon as the mixing region develops a mean temperature profile of the order of the adiabatic gradient:

$$\partial_z \overline{T} \sim \gamma. \tag{3}$$

As a consequence, once the mean profile in the bulk has reached that slope, turbulence will decline. Given γ, we can identify the adiabatic length, $L_\gamma = \Delta T/|\gamma|$ which corresponds to the prediction for the largest possible extension of the mixing layer during the RT evolution. In Fig. 4 we show the evolution of the mixing layer extension for two cases with weak (RUN A) and strong (RUN B) adiabatic gradient. Clearly, the extension of the mixing region stops to grow

when $L(t) \sim L_\gamma$. In this paper we measure the mixing layer width $L(t)$ as:

$$L(t) = 2 \int dz\, \Theta \left[\frac{\overline{T}(z,t) - T_{up}}{T_{down} - T_{up}} \right], \tag{4}$$

with $\Theta[\xi] = 2\xi;\ 0 \leq \xi \leq 1/2$ and $\Theta[\xi] = 2\,(1-\xi);\ 1/2 \leq \xi \leq 1$. The overshoot developing at the edge between turbulent and unmixed fluid is visible in Fig. 3, where we show both the nonlinear temperature inversion (inset bottom left) and the corresponding inversion in the heat flux (inset top right). This overshooting region is clearly a problem for any attempt to close the mean profile evolution with any sort of *local* eddy diffusivity:

$$\overline{u_z \theta} = -K(z,t) \partial_z \overline{T}.$$

Different models have been proposed in the literature for $K(z,t)$, going from simple homogeneous closure ($K(z,t) \propto L(t)|\dot{L}(t)|$) to Prandtl-like mixing-length closure (Biferale et al, 2011a) ($K(z,t) \propto L(t)^{5/2} \partial_z \overline{T}$) or following Spiegel's nonlinear approach (Biferale et al, 2011a) ($K(z,t) \propto L(t)^2 |\partial_z \bar{T}|^{1/2}$). All these attempts work well in the absence of overshooting and all of them suffer whenever an inversion in temperature and heat flux is observed (as in Fig. 3), implying a negative effective eddy diffusivity. In order to overcome this difficulty, we keep exact the equations for the mean profile and close only the fluctuations at the second order moments in (2). Considering $u_z \sim u$, we are left with six unknown to be defined: the three dissipative contributions on the rhs, and the three non-linear third order fluxes on the lhs. We close them adopting the simplest dimensionally-consistent *local* closure, for both fluxes and dissipative terms:

$$\begin{cases} \overline{\theta^2 u_z} = a_\theta L |\dot{L}| \partial_{zz} \overline{\theta^2}; & \epsilon_\theta = b_\theta \overline{\theta^2}/\tau(z,t) \\ \overline{(u^2+p) u_z} = a_{u_z} L |\dot{L}| \partial_{zz} \overline{u_z^2}; & \epsilon_\nu = b_{u_z} \overline{u_z^2}/\tau(z,t) \\ \overline{\theta (u_z^2 + p)} = a_{\theta u_z} L |\dot{L}| \partial_{zz} \overline{\theta u_z}; & \epsilon_{\theta,u_z} = b_{\theta u_z} \overline{\theta u_z}/\tau(z,t) \end{cases}$$

where the typical time defining the dissipation rates is fixed by $\tau(z,t) = \sqrt{\overline{u_z^2}}/L(t)$. Some comments are in order. First, we notice that the closure is now *local* but on the second order moments, i.e. *non-local* for the evolution of mean profiles. Furthermore, out of the 6 free parameters, 4 can be handled quite robustly, all the three coefficients in front of the closure for third order quantities are set $\mathcal{O}(1)$ using a first order guess from the numerics, $a_\theta = 0.2; a_{u_z} = 0.3; a_{\theta u_z} = 0.8$. Moreover, the free parameter defining the intensity of the kinetic dissipation, ϵ_ν, is less relevant in 2D (absence of direct energy cascade). It will become relevant only to define the overall long-term energy decaying once the profiles stopped (see below). The only two *delicate* free parameters are those defining the intensities of temperature and heat-flux dissipative terms, $[b_\theta, b_{\theta u_z}]$. In order to get a good agreement with the numerics we need some fine tuning for them. It is important to notice that both dissipative terms will develop a non-trivial vertical profile, i.e. they are not given by a simple bulk homogeneous parameterization.

In Fig. 4 we show that the closure is able to reproduce quantitatively the evolution of $L(t)$ for both cases of weakly stratified turbulence (A) and strongly stratified case (B). In Fig. (5) we show the capability of the model to reproduce the heat flux *vs.* temperature profile behavior, providing a sort of *aposteriori* effective eddy diffusivity. For the strong stratification case, our model is able to capture also the long time behavior, even after the evolution has come to a halt due to the adiabatic gradient, where the heat flux has completely inverted sign, see top panel of Fig. 5. In the inset of the same figure we also show the capability of the closure to reproduce the overshooting profile. As one can see the agreement is very good and the results are not very

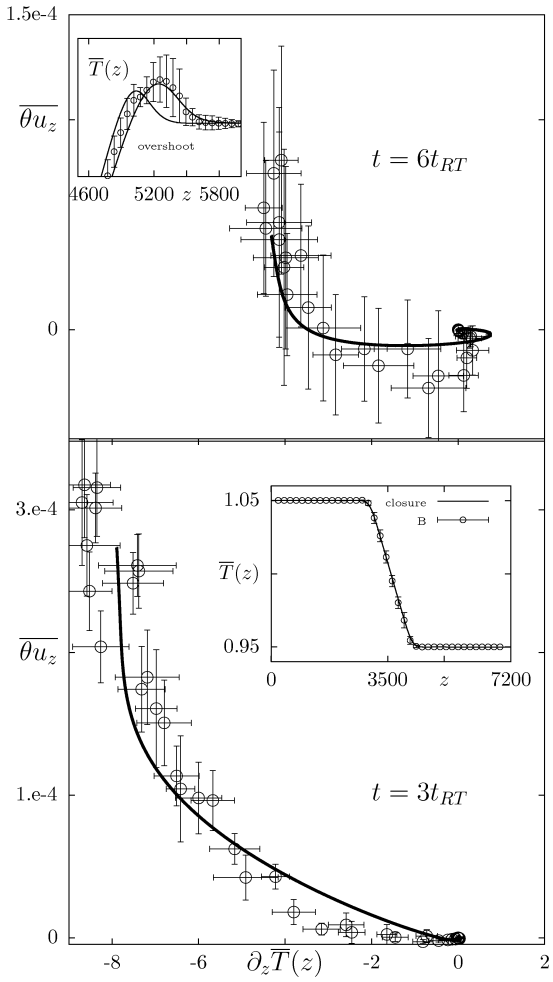

Figure 5. Check of the closure for the case with strong stratification (run B). Circles: numerical data,solid line: closure.We plot the local heat flux vs the local temperature mean gradient, $\overline{\theta u_z}$ vs $(\partial_z \overline{T}) \times 10^5$, i.e. the effective diffusivity $K(z,t)$ for two different times, $t = 3\,t_{RT}$ (bottom panel); $t = 6\,t_{RT}$ (top panel). Closure predictions ($[b_\theta, b_{\theta u_z}] = [0.35; 6.5]$) are given by the solid lines. Inset bottom panel: matching between the temperature profile and the closure. Inset top panel: overshooting region around the top boundary layer. The two lines correspond to the closure using two different choices, $[b_\theta, b_{\theta u_z}] = [0.25; 4.5]; [0.35, 6.5]$.

sensitive to the choice of the free parameters.
Once turbulence is confined away from the solid boundaries, kinetic energy in 2D is forced to decay only via *weak* viscous bulk dissipation or via temperature fluctuations, exchanging kinetic and potential energy at the boundary between turbulent and stratified flows. In Fig. 6 we show the good agreement one can get even for such asymptotic behavior using our closure model. There we compare the numerics with the outcomes of the closure using different values for the free parameters. In particular, it is evident now how the asymptotic decay is mainly dictated by the coefficient in front of the kinetic energy dissipation, the one irrelevant in an early stage of the process.

In conclusions, we have performed state-of-the-art 2D numerical simulations using a novel LBM for turbulent convection driven by a Rayleigh-Taylor instability in weakly and strongly

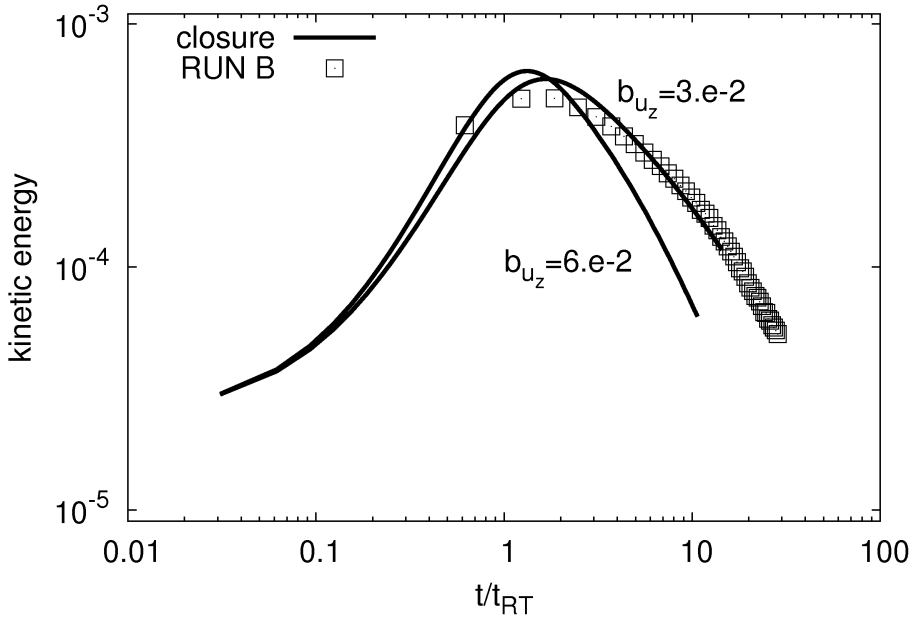

Figure 6. Log-log plot of the kinetic energy during a stratified RT evolution. The peak is reached when the profile stops. Later, energy starts to decay slowly, due to absence of viscous friction at the walls. Solid lines give the corresponding evolution in our closure obtained by keeping fixed all free parameters except for the one controlling the importance of kinetic energy dissipation, b_{u_z}. As one can notice, while the parameter is completely unimportant for the initial growth, it becomes crucial to get the correct long-time energy decaying.

stratified atmospheres. For the strongly stratified case, we are able to resolve the overshooting region with up to 800 grid points, something impossible to achieve with 3D direct numerical simulations because of lack of computing power. We have presented a second-order closure to describe the evolution of mean fields able to capture both bulk properties and the overshooting observed at the boundary between the stable and unstable regions. The closure is *local* in terms of fluctuations while keeping the evolution of the mean temperature profile exact. In order to apply the same closure to 3D cases one needs to take into account some possible non-trivial effects induced by the kinetic energy dissipation modeling, due to the presence of a forward energy cascade. As a result, also the parameter b_{u_z} will become a relevant input in the model, not only to control the very long behavior after the halt of the profile. .

We acknowledge useful discussions with G. Boffetta, A. Lawrie and A. Wirth. We acknowledge access to QPACE and eQPACE during the bring-up phase of these systems. Parts of the simulations were also performed on CASPUR under HPC Grant 2009 and 2010.

References

Belletti, F., Biferale, L., Mantovani, F., *et al* 2009 Multiphase Lattice Boltzmann on the cell Broadband Engine *Il NUovo CImento* **32**, 53.

Biferale, L., Mantovani, F., Sbragaglia, M., Scagliarini, A., Toschi, F. & Tripiccione, R. 2010 High resolution numerical study of Rayleigh-Taylor turbulence using

a lattice Boltzmann scheme. *Phys. Fluids* **22**, 115112.

Biferale, L., Mantovani, F., Sbragaglia, M., Scagliarini, A., Toschi, F., & Tripiccione, R. 2011a Second order closure in stratified turbulence: simulations and modeling of bulk and entrainment regions. *Phys. Rev. E* in press. arXiv:1101.1531.

Biferale, L., Mantovani, F., Sbragaglia, M., Scagliarini, A., Toschi, F., & Tripiccione, R. 2011b Reactive Rayleigh-Taylor systems: Front propagation and non-stationarity *Europhys. Lett.* **94**, 54004.

Boffetta, G., De Lillo, F. & Musacchio, S. 2010 Non-linear diffusion model for Rayleigh-Taylor mixing. *Phys. Rev. Lett.* **104**, 034505.

Burchard, H. & Bolding, K. 2001 Comparative analysis of four second-moment turbulence closure models for the oceanic mixed layer. *J. Phys. Oceanogr.* **31**, 1943.

Canuto, V.M. & Chistensen-Dalsgaard, J. 1998 Turbulence in astrophysics: Stars. *Annu. Rev. Fluid Mech.* **30**, 167.

Canuto, V.M., Howard, A., Cheng, Y. & Dubovikov, M.S. 2002 Ocean Turbulence. Part II: Vertical Diffusivities of Momentum, Heat, Salt, Mass, and Passive Scalars. *J. Phys. Oceanogr.* **32**, 240.

Goldrian, G., Huth, T., Krill, B., *et al* 2008 Quantum Chromodynamics Parallel Computing on the Cell Broadband Engine. *Computing in Science & Engineering* **10**, 46.

Large, W.G., McWilliams, J.C. & Doney, S.C. 1994 Oceanic vertical mixing: A review and a model with a nonlocal boundary layer parameterization. *Review Geophys.* **32**, 363.

Lawrie, A.G.W. & Dalziel, S.B. 2011 Rayleigh-Taylor mixing in an otherwise stable startification. *J. Fluid Mech.* submitted.

Ludwig, H.G., Hallard, F. & Hauschildt, P.H. 2006 Energy transport, overshoot, and mixing in the atmospheres of M-type main- and pre-main-sequence objects. *Astron. Astrophysics* **459**, 599.

Odier, P., Chen, J., Rivera, M.K. & Ecke, R.E. 2009 Fluid mixing in stratified gravity currents: the Prandtl mixing length. *Phys. Rev. Lett.* **102**, 134504.

Sbragaglia, M., Benzi, R., Biferale, L., Chen, H., Shan, X. & Succi, S. 2009 Lattice Boltzmann method with self-consistent thermo-hydrodynamic equilibria. *J. Fluid Mech* **628**, 299.

Scagliarini, A., Biferale, L., Mantovani, F., Sbragaglia, M., Sugyyama, K & Toschi, F. 2010 Lattice Boltzmann Methods for thermal flows: continuum limit and applications to compressible Rayleigh-Taylor systems. *Phys. Fluids* **22**, 055101.

Siebesma, A., Soares, P.M.M. & Teixeira, J. 2007 A Combined Eddy-Diusivity Mass-Flux approach for the convective boundary layer. *J. Atmosph. Science* **64**, 1230.

Sharp, D.H. 1984 An overview of Rayleigh-Taylor instability. *Physica D* **12**, 3.

Spiegel, E.A. 1965 Convective instability in a compressible atmosphere. *Astrophys. J.* **141**, 1068.

Trampedach, R. 2010 Convection in stellar models. *Astrophys. Space Sci.* **328**, 213.

Wirth, A. & Barnier, B. 2008 Mean circulation and structures of tilted ocean deep convection. *J. Phys. Oceanogr.* **38**, 803.